

Biophysical Journal, Volume 97

Supporting Material

Single-Molecule Study of Metalloregulator CueR–DNA Interactions Using Engineered Holliday Junctions

Nesha May Andoy, Susanta K. Sarkar, Qi Wang, Debashis Panda, Jaime J. Benítez, Aleksandr Kalininskiy, and Peng Chen

Supporting Information

To

Single-Molecule Study of Metalloregulator CueR–DNA Interactions Using Engineered Holliday Junctions

*Nesha May Andoy, Susanta K. Sarkar, Qi Wang, Debashis Panda, Jaime J. Benítez, Aleksandr Kalininskiy, and Peng Chen**

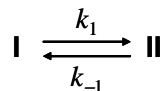
Department of Chemistry and Chemical Biology, Cornell University, Ithaca, New York 14853, U.S.A.

* To whom correspondence should be address; email: pc252@cornell.edu

I. Derivation of the single-molecule kinetics of the structural dynamics of HJC2

A. Free HJC2

The structural dynamics of a HJ, if measured at the single-molecule level at tens of milliseconds time resolution, follows a two-state kinetics effectively:



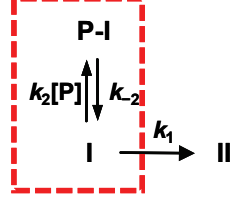
where I denotes conf-I and II denotes conf-II (see also Figure 1 in the main text). The waiting time τ_I in the E_{FRET} trajectories is the time needed to complete I \rightarrow II transition; the waiting time τ_{II} is to complete II \rightarrow I transition; both are simple one-step kinetic reactions. The probability density functions for τ_I and τ_{II} , $f_I(\tau)$ and $f_{II}(\tau)$, are both single-exponential functions, with $f_I(\tau) = k_1 \exp(-k_1 \tau)$ and $f_{II}(\tau) = k_{-1} \exp(-k_{-1} \tau)$. The inverse of the average waiting times, $\langle \tau_I \rangle^{-1}$ and $\langle \tau_{II} \rangle^{-1}$, which represent the time-averaged single-molecule rates of I \rightarrow II and II \rightarrow I transitions respectively, are:

$$\langle \tau_I \rangle^{-1} = \frac{1}{\int_0^{\infty} \tau f_I(\tau) d\tau} = k_1 \quad (\text{A1})$$

$$\langle \tau_{II} \rangle^{-1} = \frac{1}{\int_0^{\infty} \tau f_{II}(\tau) d\tau} = k_{-1} \quad (\text{A2})$$

B. Apo-CueR and HJC2 interactions

The kinetic mechanism of apo-CueR interactions with HJC2 is shown in Figure 5A. The kinetic processes happening during τ_I are the following kinetic steps:



The corresponding single-molecule rate equations are:

$$dP_{II}(t)/dt = k_1 P_I(t) \quad (B1)$$

$$dP_I(t)/dt = -(k_1 + k_2[P])P_I(t) + k_{-2}P_{P-I}(t) \quad (B2)$$

$$dP_{P-I}(t)/dt = k_2[P]P_I(t) - k_{-2}P_{P-I}(t) \quad (B3)$$

where $P(t)$'s are the probabilities of finding HJC2 in the corresponding states at time t and k 's are the rate constants for the transitions. At the on-set of each τ_1 , i.e., right after a $II \rightarrow I$ transition, the first state that HJC2 reaches is I; so the initial conditions for solving the above differential equations are: $P_I(0) = 1$, $P_{II}(0) = 0$, $P_{P-I}(0) = 0$, where $t = 0$ being the on-set of each τ_1 . And at any time, $P_I(t) + P_{II}(t) + P_{P-I}(t) = 1$.

We can then evaluate the probability density function of τ_1 , $f_1(\tau)$. The probability of finding a particular τ is $f_1(\tau)\Delta\tau$, which is equal to the probability for HJC2 to switch from I to II between τ and $\tau + \Delta\tau$, $\Delta P_{II}(\tau)$ (1, 2). Therefore, $f_1(\tau)\Delta\tau = \Delta P_{II}(\tau)$. In the limit of infinitesimal $\Delta\tau$, $f_1(\tau)$ is equal to $dP_{II}(\tau)/d\tau$. Solving for $P_{II}(\tau)$ using equations B1-B3 by Laplace transform, the probability density function of τ_1 is:

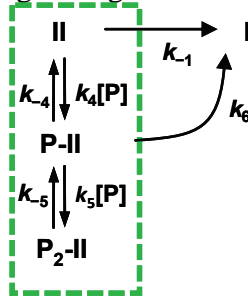
$$f_1(\tau) = \frac{k_1 e^{(\alpha+\beta)\tau}}{2\alpha} [\alpha(1 + e^{-2\alpha\tau}) + (\beta + k_{-2})(1 - e^{-2\alpha\tau})]$$

where $\alpha = -\sqrt{\frac{1}{4}(k_1 + k_{-2} + k_2[P])^2 - k_1 k_{-2}}$ and $\beta = -\frac{(k_1 + k_{-2} + k_2[P])}{2}$. Then:

$$\langle \tau_1 \rangle^{-1} = 1 / \int_0^\infty \mathcal{F}_1(\tau) d\tau = \frac{k_1}{1 + [P]/K_{P-I}}$$

where $K_{P-I} = k_{-2}/k_2$ is the dissociation constant for the apo-CueR-conf-I complex. This equation is given as Eq. 1 in the main text.

The kinetic processes happening during τ_{II} are the following kinetic steps:



The corresponding single-molecule rate equations are:

$$dP_I(t)/dt = k_{-1}P_{II}(t) + k_6P_{P-II}(t) \quad (B4)$$

$$dP_{II}(t)/dt = -(k_{-1} + k_4[P])P_{II}(t) + k_{-4}P_{P-II}(t) \quad (B5)$$

$$dP_{P-II}(t)/dt = k_4[P]P_{II}(t) - (k_{-4} + k_6 + k_5[P])P_{P-II}(t) + k_{-5}P_{P_2-II}(t) \quad (B6)$$

$$dP_{P_2-II}(t)/dt = k_5[P]P_{P-II}(t) - k_{-5}P_{P_2-II}(t) \quad (B7)$$

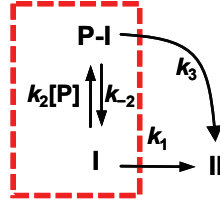
The initial conditions for solving above equations are: $P_{II}(0) = 1$, $P_I(0) = 0$, $P_{P-II}(0) = 0$, and $P_{P_2-II}(0) = 0$. And at any time, $P_I(t) + P_{II}(t) + P_{P-I}(t) + P_{P_2-II}(t) = 1$. Similarly, $f_{II}(\tau) = dP_I(\tau)/d\tau$. Using equations B4-B7 to solve for $P_I(\tau)$, we can obtain $f_{II}(\tau)$. Then,

$$\langle \tau_{II} \rangle^{-1} = 1 / \int_0^\infty \mathcal{F}_{II}(\tau) d\tau = \frac{k_{-1} + k_6[P] / K'_{P-II}}{1 + [P] / K'_{P-II} + [P]^2 / (K'_{P-II} K_{P_2-II})}$$

where $K'_{P-II} = (k_{-4} + k_6)/k_4$ and $K_{P_2-II} = k_{-5}/k_5$. This equation is given as Eq 2 in the main text.

C. Holo-CueR and HJC2 interactions.

The kinetic mechanism for holo-CueR–HJC2 interactions is shown in Figure 5B. The kinetic processes happening during τ_I are:



The corresponding single-molecule rate equations are:

$$dP_{II}(t)/dt = k_1P_I(t) + k_3P_{P-I}(t) \quad (C1)$$

$$dP_I(t)/dt = -(k_1 + k_2[P])P_I(t) + k_{-2}P_{P-I}(t) \quad (C2)$$

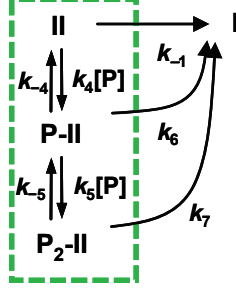
$$dP_{P-I}(t)/dt = k_2[P]P_I(t) - (k_{-2} + k_3)P_{P-I}(t) \quad (C3)$$

The initial conditions are $P_I(0) = 1$, $P_{II}(0) = 0$ and $P_{P-I}(0) = 0$ and at any time, $P_I(t) + P_{II}(t) + P_{P-I}(t) = 1$. Similarly, $f_I(\tau) = dP_{II}(\tau)/d\tau$, and solving equations C1-C3 for $P_{II}(\tau)$, we can obtain $f_I(\tau)$, and

$$\langle \tau_I \rangle^{-1} = 1 / \int_0^\infty \mathcal{F}_I(\tau) d\tau = \frac{k_1 + [P]k_3 / K'_{P-I}}{1 + [P] / K'_{P-I}}$$

where $K'_{P-I} = (k_{-2} + k_3)/k_2$. This equation is given as Eq. 3 in the main text.

The kinetic processes happening during τ_{II} are:



The corresponding single-molecule rate equations are:

$$dP_I(t)/dt = k_{-1}P_{II}(t) + k_6P_{P-II}(t) + k_7P_{P_2-II}(t) \quad (C4)$$

$$dP_{II}(t)/dt = -(k_{-1} + k_4[P])P_{II}(t) + k_{-4}P_{P-II}(t) \quad (C5)$$

$$dP_{P-II}(t)/dt = k_4[P]P_{II}(t) - (k_{-4} + k_6 + k_5[P])P_{P-II}(t) + k_{-5}P_{P_2-II}(t) \quad (C6)$$

$$dP_{P_2-II}(t)/dt = k_5[P]P_{P-II}(t) - (k_{-5} + k_7)P_{P_2-II}(t) \quad (C7)$$

The initial conditions for solving above equations are: $P_{II}(0) = 1$, $P_I(0) = 0$, $P_{P-II}(0) = 0$, and $P_{P_2-II}(0) = 0$. And at any time, $P_I(t) + P_{II}(t) + P_{P-II}(t) + P_{P_2-II}(t) = 1$. Similarly, $f_{II}(\tau) = dP_I(\tau)/d\tau$. Using equations C4-C7 to solve for $P_I(\tau)$, we can obtain $f_{II}(\tau)$ and $\langle \tau_{II} \rangle^{-1}$ for holo-CueR–HJC2 interactions.

Inconveniently, the expressions of the solutions to equations C4–C7 are so tediously complex to hamper their physical understanding. To get a clean analytical expression for $\langle \tau_{II} \rangle^{-1}$, we arbitrarily set $k_{-4} = 0$ and get:

$$\langle \tau_{II} \rangle^{-1} = \frac{k_{-1} + [P](k_{-1}k_7/(k_6K'_{P_2-II}) + k_6/K'_{P-II}) + [P]^2 k_7/(K'_{P-II}K'_{P_2-II})}{1 + [P](k_7/(k_6K'_{P_2-II}) + 1/K'_{P-II}) + [P]^2/(K'_{P-II}K'_{P_2-II})}$$

where $K'_{P-II} = k_6/k_4$ and $K'_{P_2-II} = (k_{-5} + k_7)/k_5$. This equation is given as Eq. 4 in the main text. As this equation can satisfactorily interpret the [holo-CueR] dependence of $\langle \tau_{II} \rangle^{-1}$, we use it to fit the holo-CueR data in Figure 4B to obtain other relevant kinetic parameters.

Reference

1. Xie, X. S. 2001. Single-molecule approach to enzymology. *Single Mol.* 2:229-236.
2. Xu, W., J. S. Kong, and P. Chen. Single-molecule kinetic theory of heterogeneous and enzyme catalysis. *J. Phys. Chem. C.* in press.

Supporting Figures

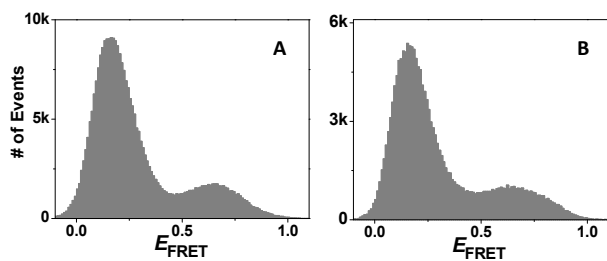


Figure S1. Histograms of HJC2 E_{FRET} trajectories in the absence (A) and presence of 1.0 μM apo-PbrR691 (B). Bin size: 0.01. Each histogram is compiled from more than 100 trajectories

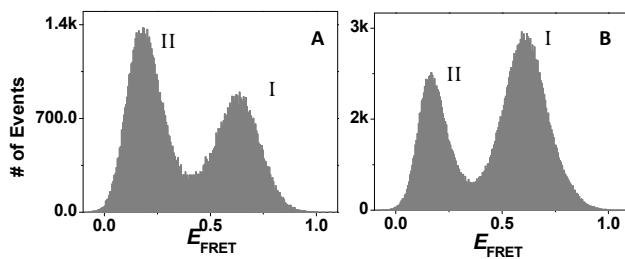


Figure S2. Histograms of HJC2 E_{FRET} trajectories in the presence of 0.5 μM apo-CueR (A) and 3 μM apo-CueR (B). Bin size: 0.005.

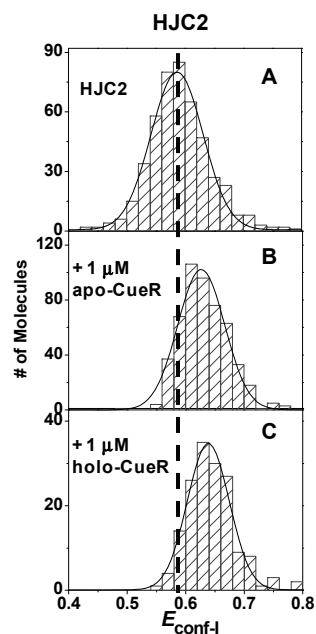


Figure S3. Histograms of $E_{\text{conf-I}}$ of HJC2 (A) in the presence of 1 μM apo-CueR (B) and 1 μM holo-CueR (C). Solid lines are Gaussian fits centered at 0.59 ± 0.01 (A), 0.63 ± 0.01 (B), and 0.64 ± 0.01 (C).

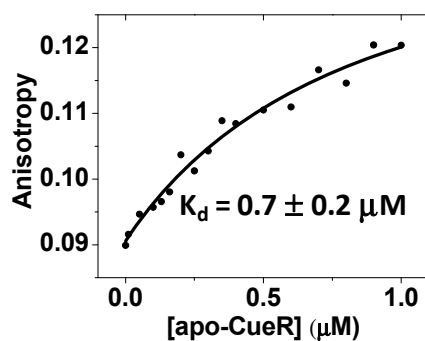


Figure S4. Fluorescence anisotropy experiment on Cy-3 labeled double-strand DNA containing only half of the dyad-symmetric sequence (5'-TGACCTTCCCCTTGCTTGGCTTGTT-3', the half sequence is underlined) titrated with apo-CueR. The solid line is the fit using Eq. 5 which gave a $K_D \sim 0.7 \mu\text{M}$.

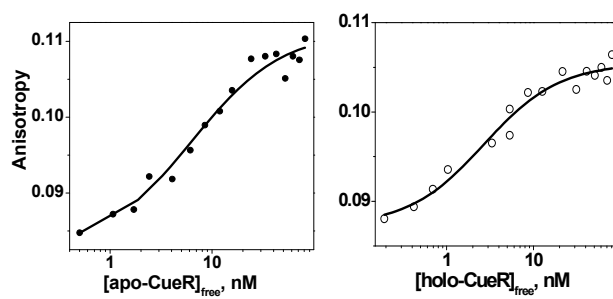


Figure S5. Data from Fig. 7 plotted against free protein concentrations.

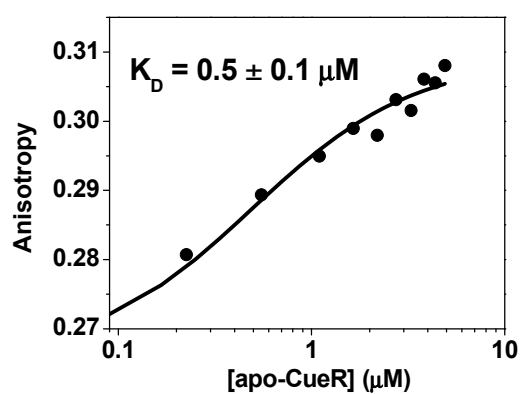


Figure S6. Fluorescence anisotropy experiment on Cy3-labeled HJC2 titrated with apo-CueR. The solid line is the fit using Eq. 5 giving a $K_D \sim 0.5 \mu\text{M}$ which is in between the affinity of apo-CueR to conf-I and to conf-II of HJC2 determined from single-molecule measurements.